Simulation of Acoustic Resonance Generated by Flow around a Long Rectangular Plate Placed in a Duct

B.T. Tan, M.C. Thompson and K. Hourigan

Department of Mechanical Engineering
Monash University, Melbourne, Victoria, 3800 AUSTRALIA

Abstract

This paper describes a numerical investigation of acoustic resonance occurring at specific flow speeds when a long rectangular plate is placed in a duct. To do this, the flow and acoustic problems are decoupled. This allows the range of flow speeds, or the associated Strouhal number (St_c), where resonance is possible to be predicted. It is shown that the Strouhal number displays a stepping behaviour as the plate length is increased. The main source or sink region where energy to transferred between the acoustic and flow fields is shown to be just downstream of the trailing edge of the plate. Visualizations show that the timing when the vortices enter this region relative to the phase of the acoustic cycle is crucial in determining if resonance can occur and is the cause of the observed stepwise increase.

Nomenclature

c	plate chord
n	integer shedding mode
P	instantaneous acoustic power transfer
$\overline{P}$	time-averaged acoustic power
Re	Reynolds number
St	Strouhal number based on thickness
St_c	Strouhal number based on chord
h	plate thickness
$\mathbf{u}$	flow velocity vector
U_∞	freestream velocity
$\mathbf{v}$	acoustic particle velocity
Δt	time step
ρ_0	mean fluid density
$\vec{\omega}$	vorticity vector

Introduction

This paper studies the flow around a long rectangular plate together with the flow-induced acoustic field when it is placed on the centreline of a duct. Besides being a coupled flow/acoustic problem of intrinsic interest, it has associated industrial applications in the fields of wind engineering, turbomachinery and heat transfer. For instance, turbomachinery devices can undergo severe related flow-induced resonant interactions between blades rows that can cause long-term fatigue or even catastrophic structural failure.

There have been numerous studies on the flow around long plates in the absence of external influences such as duct walls or an applied perturbation field. It has been found in both experimental [6, 8] and numerical studies [7, 9] that shedding from both sides of the plate are out of phase and lock to a single frequency. The Strouhal number based on chord shows a stepwise increase with increasing aspect ratio. This is a result of a feedback loop driven by vortices shed from the leading edge which later pass the trailing edge and generate a pressure pulse which in turn propagates upstream to lock further leading-edge shedding. More recent work [1] has shown the presence of strong vortices forming at the trailing edge between the passing of leading-edge vortices and it has been proposed that the

trailing-edge shedding plays a significant role in controlling the details of the feedback loop. The stepping in the Strouhal number is associated with the observed discrete increase in the number of vortex pairs between the leading and trailing edge of the plate. The hypothesized feedback loop has been previously described as an impinging leading-edge vortex instability [8, 4]. This mechanism is relatively weak and is able to lock the flow only at low Reynolds numbers ($Re < 3000$ in [6]).

At higher Reynolds numbers ($\approx 12,000$) experiments have shown that the same receptivity can be excited with small levels of crossflow sinusoidal forcing [4, 5]. Measurements of base pressure also show the frequency where the strongest base suction occurs increases in a stepwise fashion similar to that observed for the natural shedding case. Simulations, although at much lower Reynolds number ($Re = 400$), also show this behaviour [13, 14, 15]. In this case, instead of the pressure pulse from the trailing edge, the external perturbation directly locks the leading-edge shedding.

The same stepping behaviour is also observed when the plate is placed in a duct. The sketch in Figure 1 shows the setup. The plate is placed centrally with the longer axis parallel to the mean flow direction. Initially the flow is not locked and many frequencies may be present. If any of these frequencies match the resonance frequency of the duct, the acoustic mode in the duct may be excited. If the flow system is receptive to this frequency, the flow will become locked and thus complete a feedback loop, sustaining the resonance. Although it is possible to excite numerous acoustic modes in the duct, this study is only concerned with the first β-mode (as defined in [10]). This consists of a single standing wave in the crossflow direction. This field has a pressure node at the centre of the duct and an acoustic particle velocity node at the top and bottom surfaces of the duct. Earlier experiments by Welsh & Gibson [16] found two resonance ranges at $0.10 < St < 0.12$ and $0.18 < St < 0.21$ for a plate with an aspect ratio of $c/t = 5$. These different resonances were excited by slowly increasing the flow velocity until the flow field became locked to the resonant acoustic field. If the plate had an aerodynamic leading edge, there was only one resonant range [17] because there is no leading edge shedding and the flow at the trailing edge is receptive only over a narrow frequency range. Later experiments [11] for plates in the range of $0.5 < c/t < 16$ found that while certain aspect ratios displayed multiple resonant ranges, these also showed a stepwise increase with aspect ratio.
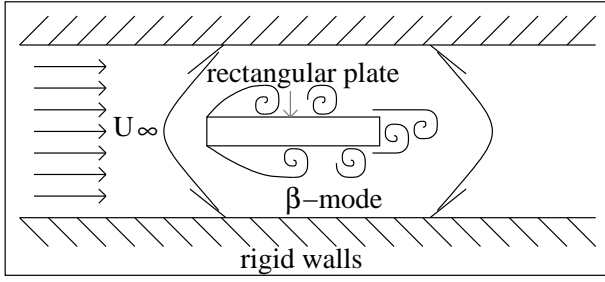
Figure 1: Schematic of the plate in a duct leading to acoustic resonance.

Numerical Technique

To treat this problem numerically the incompressible flow field and acoustic components are decoupled and treated separately. An oscillatory crossflow forcing is applied at the inlet and side boundaries of the domain for the flow solution. This mimics the effect of the resonant β-mode locally near the plate and controls the vortex shedding from the leading and trailing edges. The resonant β-mode in the duct is also calculated by solving an eigenvalue problem. Using this time-dependent resonant field, the model proposed by Howe [2, 3] is then used to determine the direction of transfer of energy between the acoustic and flow fields. According to the theory, resonance can be sustained if the transfer to the acoustic field is positive. This is only possible for certain flow velocities (or equivalent forcing Strouhal numbers).
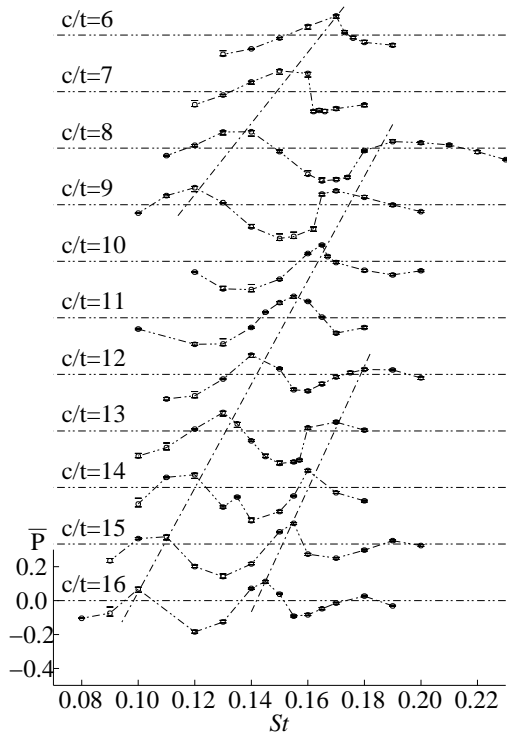

Figure 2: Time-averaged acoustic power transferred from the flow field to the sound field for plates with aspect ratios between $c/t = 6$ and 16 as a function of Strouhal number.

Simulation of the Flow Field

Simulation of the flow field involves solving the incompressible Navier-Stokes equations using a spectral-element code that has been successfully tested on a number of similar flows. The effect of the sound field on the flow is modelled through adding a 2.5% sinusoidal variation to the velocity at the inflow and side boundaries. Details of the method can be found in [13, 14, 15].
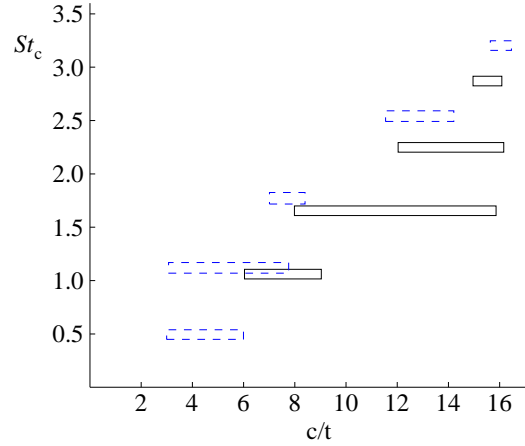

Figure 3: Strouhal number St_c ranges for which positive transfer of energy between the flow and the sound field occurs. The results of Stokes & Welsh (1988) are denoted by the dashed boxes and the numerical predictions by the solid lines.

Modeling of the Acoustic Field

Assuming the flow is in the presence of an external sound field, the theory due to Howe [2, 3] can predict the transfer of power between the flow field and the acoustic field. To sustain the resonance, the time-averaged power transfer needs to be from the flow field to the acoustic field. Although this is a necessary condition, it is not sufficient as damping may be present. Therefore these simulations may over predict the range of acoustic resonance. To perform this analysis, the integral specified in Equation 1 is evaluated on the same grid and using the same spatial scheme as the flow solver.

$$P = -\rho_0 \int \vec{\omega} \cdot (\mathbf{u} \times \mathbf{v}) dV. \tag{1}$$

In this equation, the vorticity $\vec{\omega}$, and velocity $\mathbf{u}$, are obtained from the flow solver. The remaining terms in the equation are ρ_0 the mean fluid density and $\mathbf{v}$ the acoustic particle velocity. The acoustic particle velocity is found by solving the wave equation as in [12]. This simulates the fundamental resonant acoustic field in a duct containing a plate. The spatial component can be calculated by solving an eigenvalue problem. The field is calculated on the same grid as the flow solver using the same spatial discretisation scheme. The standing wave is driven at the same frequency and phase as the forcing applied to the flow, since the later simulates the effect of the acoustic field on the flow in the vicinity of the plate.

Results

The time-averaged acoustic power transfer is calculated for plates with aspect ratios between $6 \le c/t \le 16$. The analysis is performed only within the range of duct (forcing) frequencies that locked the flow for this level of forcing. (In reality, the duct resonance frequency is fixed and the Strouhal number is

varied by changing the inflow velocity, however, this is equivalent to fixing the inflow velocity and varying the acoustic frequency. That latter approach is more convenient computationally.) Figure 2 shows the predicted values of the time-averaged acoustic energy transfer from the flow field to the acoustic field. Duct acoustic resonance can only be sustained when the values are positive. Note that many plates showed multiple frequency ranges for which resonance is possible. In addition, as the aspect ratio is increased, the frequencies at which resonance occurs also decrease as shown by the dashed lines in Figure 2. As this occurs, another resonance range develops at a higher frequency and follows the same trend.

A clearer way to view this trend is to plot the resonance range (based on chord) as a function of aspect ratio as in Figure 3. The frequency range where resonance can occur shows a stepwise increase with aspect ratio. The simulations predict that the steps are approximately $St_c = 0.55n$, for integer n. The results from Stokes and Welsh 1988 [11] are also plotted for comparison. Although both simulations and experimental results show a similar stepwise variation, the size of the step is slightly higher for the experiments (approximately $St_c = 0.6n$). This is assumed to be due to the much higher Reynolds numbers used for the experiments leading to a slightly larger effective convection velocity of the vortices.

To further understand the frequency selection of the resonance process, an attempt was made to identify the main source/sink regions of the acoustic power. To achieve this, the integration of the power integral (Equation 1) is performed but the downstream (vertical) boundary where the integration is truncated is varied. To remove the fluctuations due to the pairs of vortices further downstream, a running average is taken with an averaging length approximately the distance between a pair of vortices. The result of this is shown in Figure 4 for the cases with $c/t = 10$, and $St = 0.14$ and 0.165. In both cases, the values are approximately constant upstream of the trailing edge and further downstream. This means that there is no significant (time-averaged) power being generated in these regions. The large variation occurs just downstream of the trailing edge. This shows that there is a large sink/source in the lower/higher frequency case in this region. Analysis of numerous other cases also show the main source/sink is in the region just downstream of the trailing edge.
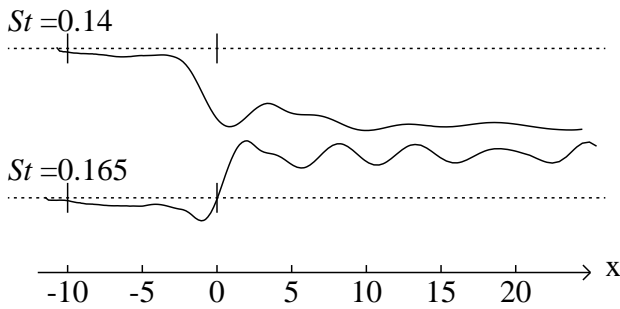
$St = 0.14$

$St = 0.165$

Figure 4: A running average of the cumulative sum in the downstream direction of the time-averaged acoustic power for a plate with $c/t = 10$ at $St = 0.14$ and $St = 0.165$. The running average is taken over approximately one wavelength of the oscillations downstream of the plate.

Figure 5 and 6 show the vorticity and instantaneous acoustic power intensity taken at 90° in the acoustic (forcing) cycle where the acoustic particle velocity (perturbation) is maximum in the upward direction. The acoustic power intensity is
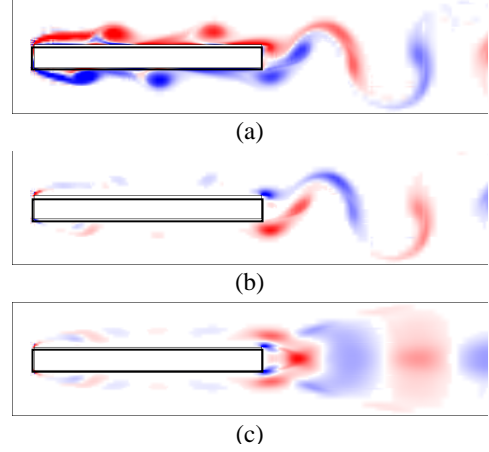

(a)

(b)

(c)

Figure 5: Visualisations for $c/t = 10$ and $St = 0.14$. (a) Vorticity plots taken at 90° in the cycle. (b) Instantaneous acoustic power also at 90° in the cycle. (c) Time-averaged acoustic power. (Note: (b) and (c) are extracted from the integrand of Equation 1. Blue and red represent positive and negative regions respectively.

obtained by calculating the value of the integrand on the right hand side of Equation 1. At a duct frequency of $St = 0.14$, as in Figure 5, resonance could not be sustained because the nett transfer of energy is from the acoustic field to the flow field. The opposite occurs in Figure 6 ($St = 0.165$) and the system could sustain an acoustic resonance. The main difference between these two flows is the phase of the vortices entering the region just downstream of the trailing edge. In the lower frequency case, the main vortical structures just downstream of the trailing edge are clockwise vortices (one from the leading edge and another generated at the trailing edge). At the higher frequency, the top (anti-clockwise) vortices are just entering the wake. Based on the integrand in Equation 1, with the flow from left to right and the acoustic particle velocity upwards, vortices with a clockwise/anti-clockwise sense result in negative/positive transfer of energy between the flow field and the acoustic field. As vortices are shed from the opposing side when the acoustic particle velocity is in the downward direction during the second half of the cycle, the same behavior can be expected.

It is now possible to explain the trend in resonance ranges discussed earlier. With the flow locked to the sound (forcing) field, the frequency of the excitation controls the rate at which vorticity is generated at the leading edge. As the convection velocity of these vortices is relatively independent of forcing frequency and amplitude [14], the arrival at the trailing edge is governed by aspect ratio but the phase of the acoustic cycle will then be a function of frequency. The stepwise increase in frequency (St_c) range where the system resonates is so that the flow maintains this favorable phase. For each step, as the aspect ratio increases more time is required for the leading edge vortices to reach the trailing edge. Therefore a proportionally lower frequency is required to keep the same phase relationship so that the energy transfer to the acoustic field is positive. Thus the Strouhal number based on chord ($St_c = cf/U_\infty$) remains constant. In fact, St_c/n is the average convective velocity of the vortices along the plate. Each successively higher step corresponds to an extra pair of vortices along the plate just as in the natural shedding case [6] and the forced shedding case [13].
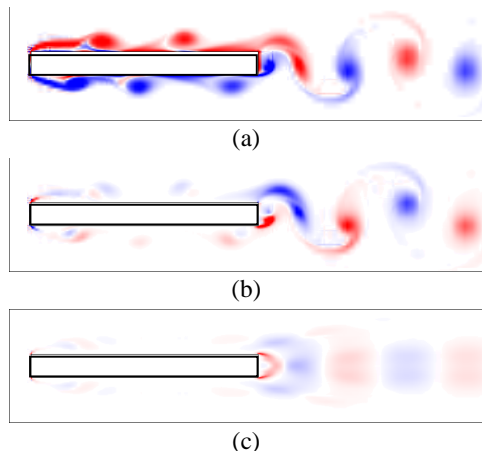
Figure 6: As for Figure 5, except for $St = 0.165$

Conclusion

The simulation of the flow field together with the modeling of the acoustic field is able to predict the Strouhal number ranges for which resonance occurs in good agreement with experimental observations. The main source/sink of acoustic energy results from the region near the trailing edge as leading-edge vortices pass over the trailing edge into the wake. The crucial element in sustaining the acoustic resonance is the relative phase between the vortices entering the wake and the acoustic (forcing) field. This results in the Strouhal number ranges for which resonance occurs displaying a stepwise increase with aspect ratio.

Acknowledgments

References

[1] Hourigan K., Thompson M.C. and Tan B.T., Self-sustained Oscillations in Flows around Long Blunt Plates, *J. Fluids Struct.*, **15** (3/4), 2001, 387–398.

[2] Howe M.S., Contributions to the Theory of Aerodynamic Sound, with Applications to Excess Jet Noise and the Theory of the Flute, *J. Fluid Mech.*, **71**, 1975, 625–673.

[3] Howe M.S., The Dissipation of Sound at an Edge, *J. Sound Vib.*, **70**, 1980, 407–411.

[4] Mills R., Sheridan J., Hourigan K. and Welsh M.C. The Mechanism Controlling Vortex Shedding from Rectangular Bluff Bodies, *12th Australasian Fluid Mechanics Conference*, editor R.W. Bilger, 1995, 227–230.

[5] Mills R., Hourigan K. and Sheridan J. Response of Base Suction and Vortex Shedding From Rectangular Prisms, *Journal of Fluid Mechanics*, 2001, submitted.

[6] Nakamura Y., Ohya Y. and Tsuruta H., Experiments on Vortex Shedding from Flat Plates with Square Leading and Trailing Edges, *J. Fluid Mech.*, **222**, 1991, 437–447.

[7] Nakayama R., Nakamura Y., Ohya Y. and Ozono S., A Numerical Study of the Flow around Flat Plates at low Reynolds Numbers, *J. Wind Eng. Ind. Aerodyn.*, **46 & 47**, 1993, 255–264.

[8] Naudascher E. and Wang Y., Flow-Induced Vibration of Prismatic Bodies and Grids of Prisms, *J. Fluid Struct.*, **7**, 1993, 341–373.

[9] Ohya Y., Nakamura Y., Ozono S., Tsuruta H. and Nakayama R., A Numerical Study of Vortex Shedding from Flat Plates with Square Leading and Trailing Edges, *J. Fluid Mech.*, **236**, 1992, 445–460.

[10] Parker R., Resonant Effects in Wake Shedding from Parallel Plates: Some Experimental Observations, *J. Sound Vib.*, **4**, 1966, 62–72.

[11] Stokes A.N. and Welsh M.C., Sound Interaction in a Duct Containing a Plate, Part II: Square Leading Edge, *J. Sound Vib.*, **104**(1), 1986, 55–73.

[12] Stoneman S.A.T., Hourigan K., Stokes A.N. and Welsh M.C., Resonant Sound caused by Flow Past Two Plates in Tandem in a Duct, *J. Fluid Mech.*, **192**, 1988, 455–484.

[13] Tan B.T., Thompson M.C. and Hourigan K., Simulated Flow around Long Rectangular Plates under Cross Flow Perturbations, *Int. J. Fluid Dynamics*, **2**, 1998, Article 1.

[14] Tan B.T., Thompson M.C. and Hourigan K. Simulation of Perturbed Flow around a Rectangular Cylinder, *Proceedings of the ASME Fluids Engineering Division Summer Meeting*, 1998.

[15] Tan B.T., Thompson M.C. and Hourigan K. Numerical Predictions of Forces on a Long Rectangular Plate Subjected to Cross-Flow Perturbation, *13th Australasian Fluid Mechanics Conference*, (editors M.C. Thompson and Hourigan K., 1998, 789–794.

[16] Welsh & Gibson, Interaction of Induced Sound with Flow Past a Square Leading Edged Plate in a Duct, *J. Sound Vib.*, **67**(4), 1979, 501–511.

[17] Welsh M.C., Stokes A.N. and Parker R. Flow-Resonant Sound Interaction in a Duct Containing a Plate, Part I: Semi-circular Leading Edge, *J. Sound Vib.*, **95**(3), 1984, 305–323.